

Synthesis of an Artificial High Effective Permittivity Medium in a SIW Periodically Loaded with Metallic Cylinders

G. Vicent, Á. Coves, E. Bronchalo, and G. Torregrosa

Departamento de Ingeniería de Comunicaciones, Universidad Miguel Hernández de Elche, Spain

Abstract— Recently, a new topology of step-impedance bandpass filters in Substrate Integrated Waveguide (SIW) technology has been theoretically and experimentally demonstrated in which the high impedance regions, i.e., those with low effective permittivity, have been achieved by inserting air holes to lower the substrate permittivity. Going a step further, in this work we propose a different way to obtain a high-low permittivity step in a SIW, by increasing the relative permittivity in some regions. This can be practically achieved by inserting in the dielectric an array of metallic inclusions. This paper presents the results of a systematic study of the effective permittivity in a SIW in which arrays of metallic cylinders are added along the waveguide in order to synthesize a higher effective permittivity. The study has been performed with the commercial software tool Ansys High Frequency Structural Simulator (HFSS). The results of this study will be used in a new topology of bandpass filters in SIW technology based on coupled cavities of different permittivity, achieved by the introduction of metallic cylinders in the higher permittivity sections and air holes in the lower ones.

1. INTRODUCTION

After the first works on Substrate Integrated Waveguide (SIW) [1, 2], many papers have been published on this transmission medium which takes the advantages of planar lines for easy integration with other circuits, and low radiation losses of waveguides. This technology has been used for making a number of microwave devices such as filters, diplexers, couplers and antennas, among others [3–5]. Recently, a new topology of step-impedance bandpass filters in SIW technology has been theoretically and experimentally demonstrated [6]. The high impedance regions, i.e., those with low effective permittivity, have been achieved by inserting air holes to lower the substrate permittivity. However, there is a natural limit in the low effective permittivity obtained in the perforated regions, given by the maximum volume of dielectric material that can be removed, and the air hole positions in the waveguide. In [6], a reduction of the relative permittivity in a perforated SIW waveguide of 42% was achieved, which was theoretically and experimentally demonstrated. Going a step further, in this work we propose a different way to obtain a high-low permittivity step in a SIW, by increasing the relative permittivity in some regions. This can be practically achieved by inserting in the dielectric an array of metallic inclusions, as demonstrated in previous works [7, 8]. This paper presents the numerical results of a study of the effective permittivity in a SIW in which an array of metallic cylinders has been inserted to synthesize a higher effective permittivity. The study has been performed by using the commercial software tool Ansys High Frequency Structural Simulator (HFSS). For each analyzed geometry, only one period along the propagation direction is simulated, and by applying periodic conditions at each edge of the periodic cell, the obtained cutoff frequency of the waveguide provides its effective permittivity. Several insertion densities have been simulated to study the influence of the metal/dielectric volume relation in the effective permittivity. The results of this study will be used in a new topology of bandpass filters in SIW technology based on coupled cavities of different permittivity, achieved by the introduction of metallic cylinders in the higher permittivity sections and air holes in the lower ones.

2. STUDY OF THE EFFECTIVE PERMITTIVITY OF A SIW WITH PERIODIC METALLIC CYLINDERS

Figure 1(a) shows the scheme of a section of the waveguide under study, consisting of a conventional SIW in which an array of metallic cylinders are added along the waveguide propagation region, in this case with a triangular pattern. This waveguide is constituted by two rows of parallel metallic posts (or via holes) delimiting the area of propagation of the fundamental TE_{10} mode of the SIW. The metallic posts are characterized by their separation s_v , and by their diameter d_v , whose values must be appropriately chosen in order to avoid radiation losses. The propagation constant of this guide is determined by the width a_{SIW} (see Fig. 1(a)) of the SIW, and also by the effective permittivity obtained after the insertion of the metallic cylinders in the propagation area. In our

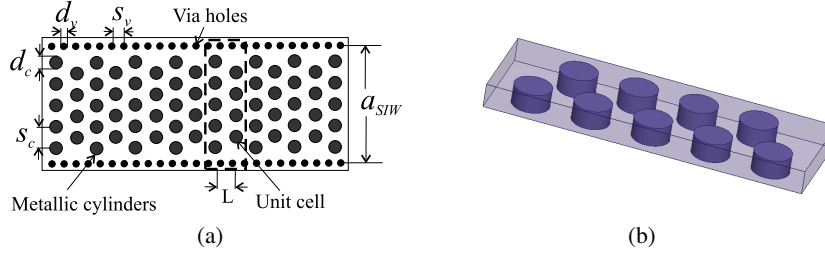


Figure 1: (a) Section of a SIW structure with periodic metallic cylinders. (b) Unit cell of the equivalent rectangular waveguide filled with periodic metallic cylinders.

case, the value of the waveguide height is $b = 0.63 \text{ mm}$, corresponding to the thickness of the substrate employed—Taconic CER-10—. The metallic cylinders are characterized by their diameter d_c , separation s_c , and height h , whose choice will determine the electromagnetic behavior in the waveguide. Their values will be limited by the availability of drills in the manufacturing process on one hand, and by the minimum separation between the edges of adjacent cylinders, which will be fixed to $200 \mu\text{m}$, in order to ensure a certain mechanical strength. On the other hand, the height h of the metallic cylinders must be lower than, but not far from the waveguide height b , in order to achieve a high effective permittivity in the waveguide.

A previous study [9] demonstrates that a SIW can be analyzed as an equivalent rectangular waveguide of effective width a given by:

$$a = a_{SIW} - \frac{d_v^2}{0.95s_v} \quad (1)$$

Therefore, all the study performed in this section is carried out using such equivalent waveguide of width a given by Eq. (1), and height b .

In order to characterize the electromagnetic field propagation in a waveguide with periodic metallic cylinders, the commercial software tool Ansys HFSS has been employed. The eigenmode module of such analysis tool yields the cutoff frequencies of the modes of a periodic waveguide of unit cell L (see Fig. 1(a)) with a phase delay ϕ between its unit cell planes, which can be directly related to its propagation constant β :

$$\beta L = \phi. \quad (2)$$

The particular phase shift $\phi = 0$ yields the cutoff frequency of the modes. Therefore, the dispersion curve of the waveguide modes can be easily obtained by performing a phase delay sweep. We have restricted our study to the monomode regime of the waveguide. In this case, for designing purposes, it is interesting to define an equivalent dielectric homogeneous waveguide whose effective permittivity is related to the cutoff frequency of its TE_{10} mode through the following expression:

$$\varepsilon_{\text{ref}} = \frac{c^2}{4a_{\text{eff}}^2 f_c^2} \quad (3)$$

where c is the speed of light in free space and f_c is the cutoff frequency of the first waveguide mode provided by the simulation software.

3. SIMULATION RESULTS

Using Eq. (4) derived in the previous section, we have obtained the effective relative permittivity of a rectangular waveguide of dimensions $a = 8.5 \text{ mm}$ and $b = 0.63 \text{ mm}$ (being b the height of the substrate employed—Taconic CER-10—, with $\varepsilon_r = 10$ and $\tan \delta = 0.0035$), periodically filled with a triangular pattern of metallic cylinders along the waveguide, with 9 cylinders of height $h = 4/5 b$ in the periodic cell of length $L = 2.771 \text{ mm}$ for this particular configuration (see Fig. 1(b)).

Firstly, we have obtained the effective permittivity of this rectangular waveguide periodically filled with 9 metallic cylinders, with a fixed distance between their centers of $s_c = 1.6 \text{ mm}$. Following the procedure described in the last section, the cutoff frequency of the fundamental mode of this waveguide provides its effective permittivity. In Fig. 2 it is represented the effective permittivity of this waveguide as a function of the diameter d_c of the metallic cylinders. It can be seen that ε_{ref} varies from the substrate permittivity $\varepsilon_{\text{ref}} = 10$ (when $d_c = 0$, i.e., for the case without metallic

cylinders) up to 22.8 (for $d_c = 1.1$ mm). This graph can be employed to synthesize a desired ϵ_{ref} for a filter design.

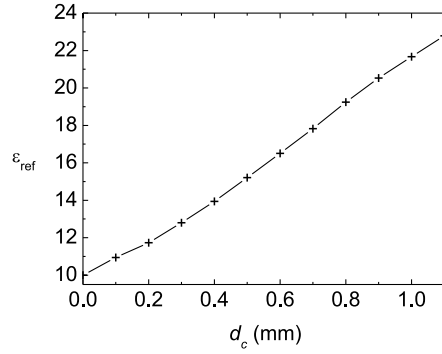


Figure 2: ϵ_{ref} of a SIW filled with periodic metallic cylinders as a function of their diameter d_c , for a fixed value between their centers $s_c = 1.6$ mm.

Next, we have analyzed the variation of the effective permittivity with the distance between cylinders, for a fixed diameter $d_c = 1.1$ mm. In Fig. 3 it is represented the effective permittivity of this waveguide as a function of the distance between the metallic cylinders s_c from 1.3 mm (corresponding to a minimum distance between the edges of adjacent cylinders of 200 μm , in order to ensure a certain mechanical strength) to 1.7 mm (distance between the edges of 600 μm). Again, this graph allows to synthesize a desired ϵ_{ref} for a filter design.

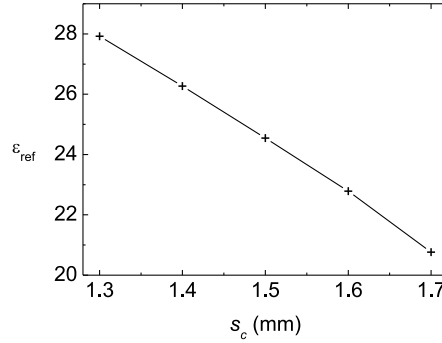


Figure 3: ϵ_{ref} of a SIW filled with periodic metallic cylinders as a function of their distance s_c , for a fixed diameter $d_c = 1.1$ mm.

At the sight of the previous results, we have chosen an implementable configuration of $d_c = 1.1$ mm and $s_c = 1.6$ mm (with a distance between the edges of 0.5 mm), which yields an effective permittivity $\epsilon_{\text{ref}} = 22.8$. For this configuration, following the procedure described above (see Eq. (2)), we have computed the dispersion diagram of the periodically filled waveguide with metallic cylinders. In Fig. 4 it is compared the dispersion curve of the periodically filled waveguide with metallic cylinders for $d_c = 1.1$ mm and $s_c = 1.6$ mm (crosses) with that of its equivalent dielectric homogeneous waveguide (solid line) of $\epsilon_{\text{ref}} = 22.8$. In this figure, it can be checked that the effective permittivity equivalence is only strictly satisfied at cutoff, given the frequency dependent nature of the metallic inclusions. However, the equivalence can be used as a first approximation in the filter design.

Finally, in order to check the validity of the previous results, we have analyzed the dispersion behaviour of a periodically filled SIW with metallic cylinders. For this purpose, we have obtained the equivalent rectangular width in SIW technology a_{SIW} , and we have designed microstrip to SIW transitions. To this aim, the following parameters for the via holes have been employed: $d_v = 0.7$ mm, $s_v = 0.95$ mm, which provide a SIW width $a_{\text{SIW}} = 9.2$ mm. On the other hand, for the microstrip to SIW transition, the same transition presented in [2] has been implemented, consisting of a microstrip taper (see Fig. 5), whose dimensions W_t and L_t have been optimized for a maximum matching of the waveguide transitions, while the width of the microstrip line is of 0.6 mm (50 Ω). In Fig. 6 there are shown the scattering parameters of a 46 mm length section of the periodically filled SIW with metallic cylinders under study (including dielectric and conductor

losses -copper-) obtained with the modal module of Ansys HFSS, showing a cutoff frequency of $f_c = 3.68$ GHz, which is very similar to the value obtained of 3.70 GHz with the eigenmode module of Ansys HFSS for the same waveguide configuration.

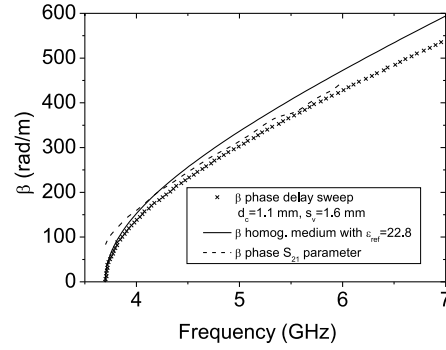


Figure 4: Comparison of the dispersion curve of the periodically filled waveguide with metallic cylinders for $d_c = 1.1$ mm and $s_c = 1.6$ mm (crosses) with that of its equivalent dielectric homogeneous waveguide (solid line) of $\epsilon_{\text{ref}} = 22.8$.

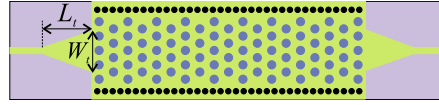


Figure 5: Scheme of a periodically filled SIW with metallic cylinders.

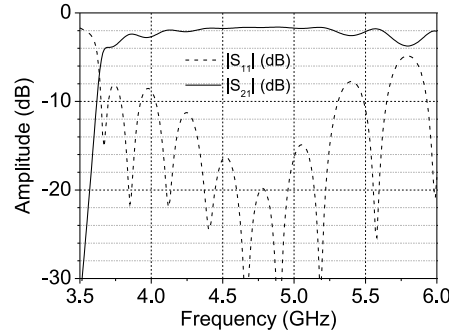


Figure 6: Simulated frequency response of a SIW section of width $a = 9.2$ mm and length $l = 46$ mm periodically filled with metallic cylinders of parameters: $d_c = 1.1$ mm and $s_c = 1.6$ mm.

Finally, the dispersion curve of the SIW waveguide periodically filled with metallic cylinders whose electrical response is shown in Fig. 6 has been computed from its scattering parameters obtained for two different lengths using the approach presented in [2]. The simulated dispersion curve obtained by this method is represented in Fig. 4 with dashed line, showing a good agreement in the represented operation band. All the theoretical analysis performed in this work is going to be experimentally verified shortly.

4. THEORETICAL MODELING AND COMPARISON WITH SIMULATIONS

A theoretical model of the artificial propagation medium is convenient to provide a better understanding of the electromagnetic problem and helpful insight for designing new devices. The theoretical study of artificial dielectrics began early in the history of electromagnetism [10]. Some particular problems have been solved in the context of electrostatics, as the one that we have chosen to model the propagation in the cylinder-loaded SIW: a tetragonal array of conducting cylinders oriented along one of the array axis and with the external electric field parallel to the cylinders. The effective permittivity relative to the host medium permittivity $\tilde{\epsilon}_{\text{ref}}$ is given by [11]

$$\tilde{\epsilon}_{\text{ref}} = 1 + \frac{N\alpha/\epsilon_0}{1 - C\alpha/\epsilon_0}. \quad (4)$$

where α is the polarizability of the inclusions, N the number of inclusions per unit volume, and C is an interaction constant providing the correction to the external electric field due to the dipoles surrounding the dipole under consideration. For an infinite tetragonal network of dipoles, the interaction constant is given by [11]

$$C = \frac{1}{l_y^3} \left\{ \frac{1.202}{\pi} - 16\pi K_0 \left(\frac{2\pi l_t}{l_y} \right) \right\} \quad (5)$$

In this expression, Y is the axis parallel to the external electric field, the l_k are the unit cell dimensions along the axes (l_t is the transverse dimension along X and Z axes), and K_0 is the modified Bessel function of second kind and zero order.

Applying the image theory to the waveguide walls allows us to represent the waveguide as an infinite dipole array. We will place just a layer of cylindrical insertions parallel to the wider side of the waveguide. Therefore, $l_y = b$ in Eq. (5), being b the height of the waveguide.

Referring the polarizability of a perfectly conducting cylinder, we have followed the paper of Taylor [12]. The polarizability for the field oriented along the cylinder axis is given by

$$\frac{\alpha}{\varepsilon_0 V_0} = \frac{2h}{D} \left[\frac{r_b}{3} + r_0 \frac{\Gamma(3/2)}{2^{2/3} \Gamma(13/6)} \right] + t_b + t_0 \frac{2^{1/3}}{\Gamma(5/3)} \quad (6)$$

where h is the height of the cylinder, D its diameter and V_0 its volume, and where the parameters r_b , r_0 , t_b and t_0 depend on the aspect ratio h/D [12]. For the substrate presented in the preceding sections, with $b = 0.63$ mm, we have chosen as feasible dimensions $h = D = 0.5$ mm. We have simulated with Ansys HFSS a waveguide with $a = 10$ mm and several densities of inclusions: 4 to 9 cylinders along the wider side of the waveguide, corresponding to l_t between 1.1 and 2.5 mm. We have left a distance $l_t/2$ from the outermost cylinders to the vertical walls of the waveguide to get the same spacing up to the first image dipole formed by these walls. The effective permittivity of this transmission media have been obtained from the simulation by the method explained in Section 2.

The results are compared with the predictions of the theoretical model expressed by formulas (4)–(6) in Fig. 7. It is clear that the model predictions scale much faster with the density of inclusions. This divergence could be due to several causes: 1) The dipole approximation may be inadequate for high inclusion densities; 2) The inhomogeneity of the electric field for the guided mode is not considered in the model; 3) The theoretical model is electrostatic, while the propagating mode is electromagnetic. Those aspects of the problem are now under consideration to elaborate a more sophisticated model for the SIW effective permittivity.

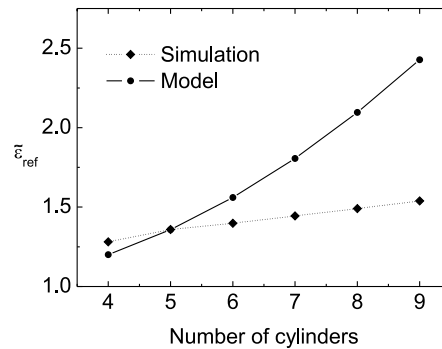


Figure 7: Effective permittivity relative to the host medium permittivity of a waveguide loaded with conducting cylinders: results of Ansys HFSS simulation and theoretical model (see text).

5. CONCLUSION

In this work it is proposed a new way to increase the permittivity in a SIW by inserting a periodic array of metallic cylinders along the waveguide. A systematic study of the resulting effective permittivity has been performed as a function of the cylinders diameter and separation. The results of this study have been numerically checked through simulations of the electrical response of a particular design of a SIW filled with metallic cylinders. A theoretical model, based on

electrostatic calculations and a dipole approximation for the field created by the cylinders, has been tested against simulation results. The results indicate that a more sophisticated approach is needed to describe theoretically the effective permittivity of the medium.

ACKNOWLEDGMENT

This work was supported by the Agencia Estatal de Investigación (AEI) and by the Unión Europea through the Fondo Europeo de Desarrollo Regional — FEDER — “Una manera de hacer Europa” (AEI/FEDER, UE), under the Research Project TEC2016-75934-C4-2-R.

REFERENCES

1. Uchimura, H., T. Takenoshita, and M. Fujii, “Development of a laminated waveguide,” *IEEE Trans. Microw. Theory Tech.*, Vol. 46, No. 12, 2438–2443, 1998.
2. Deslandes, D. and K. Wu, “Integrated microstrip and rectangular waveguide in planar form,” *IEEE Microw. Wireless Comp. Lett.*, Vol. 11, No. 2, 68–70, 2001.
3. Yan, L., W. Hong, G. Hua, J. Chen, K. Wu, and T. J. Cui, “Simulation and experiment on SIW slot array antennas,” *IEEE Microw. Wirel. Comp. Lett.*, Vol. 14, No. 9, 446–448, 2004.
4. Chen, X. P., K. Wu, and Z. L. Li, “Dual-band and triple-band substrate integrated waveguide filters with Chebyshev and quasielliptic responses,” *IEEE Trans. Microw. Theory Tech.*, Vol. 55, No. 12, 2569–2578, 2007.
5. Bozzi, M., A. Georgiadis, and K. Wu, “Review of substrate integrated waveguide (siw) circuits and antennas,” *IET Microw. Antennas Prop.*, Vol. 5, No. 8, 909–920, 2011.
6. Coves, A., G. Torregrosa, A. A. San Blas, M. A. Sánchez-Soriano, A. Martellosio, E. Bronchalo, and M. Bozzi, “A novel band-pass filter based on a periodically drilled SIW structure,” *Radio Science*, Vol. 51, 328–336, 2016.
7. Nguyen, H. V., J. Gauthier, J. M. Fernández, M. Sierra-Castañer, and C. Caloz, “Metallic wire substrate (MWS) for miniaturization in planar microwave applications,” *Proceedings of Asia-Pacific Microwave Conference*, 1084–1087, Yokohama, Japan, December 2006.
8. Njoku, C. C., W. G. Whittow, and J. C. Vardaxoglou, “Simulation methodology for synthesis of antenna substrates with microscale inclusions,” *IEEE Trans. Antennas and Prop.*, Vol. 60, No. 5, 2194–2204, 2012.
9. Cassivi, Y., L. Perreggini, P. Arcioni, M. Bressan, K. Wu, and G. Conciauro, “Dispersion characteristics of substrate integrated rectangular waveguide,” *IEEE Microw. Wirel. Compon. Lett.*, Vol. 12, No. 9, 333–335, 2002.
10. Kharadly, M. M. Z. and W. Jackson, “The properties of artificial dielectrics comprising arrays of conducting elements,” *Proc. of the IEE - Part III: Radio and Commun. Engin.*, Vol. 100, No. 66, 199–212, 1953.
11. Collin, R. E., *Field Theory of Guided Waves*, Wiley-IEEE Press, 1990.
12. Taylor, T. T., “Electric polarizability of a short right circular conducting cylinder,” *J. Research of the National Bureau of Standards — B. Mathematics and Mathem. Phys.*, Vol. 64B, No. 3, 135–143, 1960.